

High-Precision Measurement of Sine and Pulse Reference Signals using Software-Defined Radio

Carsten Andrich*, Alexander Ihlow†, Julia Bauer*, Niklas Beuster†, Giovanni Del Galdo*†

*Fraunhofer Institute for Integrated Circuits IIS, 98693 Ilmenau, Germany

†Institute for Information Technology, Technische Universität Ilmenau, 98693 Ilmenau, Germany

Phone: +49 3677 69-4281, Email: carsten dot andrich at iis dot fraunhofer dot de

Abstract—This paper addresses simultaneous, high-precision measurement and analysis of generic reference signals by using inexpensive commercial off-the-shelf Software Defined Radio hardware. Sine reference signals are digitally down-converted to baseband for the analysis of phase deviations. Hereby, we compare the precision of the fixed-point hardware Digital Signal Processing chain with a custom Single Instruction Multiple Data (SIMD) x86 floating-point implementation. Pulse reference signals are analyzed by a software trigger that precisely locates the time where the slope passes a certain threshold. The measurement system is implemented and verified using the Universal Software Radio Peripheral (USRP) N210 by Ettus Research LLC. Applying standard 10 MHz and 1 PPS reference signals for testing, a measurement precision (standard deviation) of 0.36 ps and 16.6 ps is obtained, respectively. In connection with standard PC hardware, the system allows long-term acquisition and storage of measurement data over several weeks. A comparison is given to the Dual Mixer Time Difference (DMTD) and Time Interval Counter (TIC), which are state-of-the-art measurement methods for sine and pulse signal analysis, respectively. Furthermore, we show that our proposed USRP-based approach outperforms measurements with a high-grade Digital Sampling Oscilloscope.

Index Terms—Phase Measurement, Time Measurement, Digital Signal Processing, Measurement Techniques, Software Defined Radio, Computerized Instrumentation, Reference Signal, 10 MHz, 1 Pulse Per Second (1 PPS), Time Domain Analysis, Time Interval Counter (TIC), Dual Mixer Time Difference (DMTD).

I. INTRODUCTION

REFERENCE signals are relied upon, when electronic measurements are required to meet demanding timing or frequency precision constraints. Either a single device can be coupled with a more accurate external reference, or multiple devices can be synchronized using an appropriately distributed reference signal. A particularly challenging example is the synchronization of a spatially distributed measurement setup, necessitating the use of multiple references, one for each location of the measurement.

Exemplary frequency standards used to generate highly precise reference signals are atomic clocks or GPS Disciplined Oscillators (GPSDO). These standards usually output both a sine wave and a pulse signal, while lab-grade measurement devices have inputs for both signal types.

A. Sine Wave Reference Signal

A simplified sine wave reference signal model is given by Equation 1, consisting only of a perfect sine wave at the reference frequency f_r and a time-variant phase error term $\varphi_e(t)$, neglecting signal levels and noise [1].

$$x_{\text{sine}}(t) = \sin(2\pi f_r t + \varphi_e(t)) \quad (1)$$

Sine wave reference signals are used for *relative* time synchronization, meaning that no drift between the time base of the reference signal and the time base of the synchronized system will occur. This is usually achieved by using a Phase Locked Loop (PLL) to lock the internal clock of the measurement system to the reference signal. In case of Radio Frequency (RF) measurement devices, local oscillators may also be locked to the reference signal to improve their frequency accuracy or to enable RF phase coherence.

The reference frequency f_r may depend on the intended application, but 10 MHz signals enjoy widespread device support, with 5 MHz and 100 MHz being alternative choices. Although most applications rely on sine waves, some may use rectangular signals instead. Fortunately, all considerations for sine waves apply to rectangular signals as well, since the latter can be transformed into the former by means of a band-pass filter.

Due to their periodic nature, sine (and rectangular) reference signals cannot provide an absolute time base. For this purpose, a trigger event is needed, i.e. a Pulse Reference Signal.

B. Pulse Reference Signal

A simplified pulse signal model is given by Equation 2, consisting of a pulse waveform $\text{pls}(t)$ convolved with an infinite series of Dirac pulses $\delta(t)$, which are equally spaced T_{period} apart, except for a time error $t_e[n]$.

$$x_{\text{pulse}}(t) = \text{pls}(t) * \sum_{n=-\infty}^{\infty} \delta(t - n \cdot T_{\text{period}} - t_e[n]) \quad (2)$$

The signal's timing accuracy depends on its rise-time [2], which is inversely proportional to its bandwidth. As signal bandwidth is always finite and free of discontinuities (i.e. no rectangular band-limitation), a simple $\text{pls}(t)$ signal model is given by the 2nd order low-pass characteristic. This model may be an oversimplification, but it shows two typical characteristics of pulse signals, namely a finite rise-time and transient overshoots.

We will model a single edge of $\text{pls}(t)$ using the 2nd order low-pass step response $h_{\text{LP2}}(t)$, with the angular cutoff frequency ω_0 and the damping coefficient ζ :

$$h_{\text{LP2}}(t) = 1 - \frac{1}{\sqrt{1 - \zeta^2}} \cdot e^{-\zeta\omega_0 t} \cdot \sin\left(\sqrt{1 - \zeta^2} \omega_0 t + \arccos(\zeta)\right)$$

Based on said step response, a single pulse with high-level duration T_{high} will be modeled as follows, again disregarding signal amplitude (see Figure 1 for an example):

$$\text{pls}(t) = \begin{cases} 0, & \text{if } t < 0 \\ h_{\text{LP2}}(t), & \text{if } 0 \leq t < T_{\text{high}} \\ h_{\text{LP2}}(t) - h_{\text{LP2}}(t - T_{\text{high}}), & \text{if } t \geq T_{\text{high}} \end{cases}$$

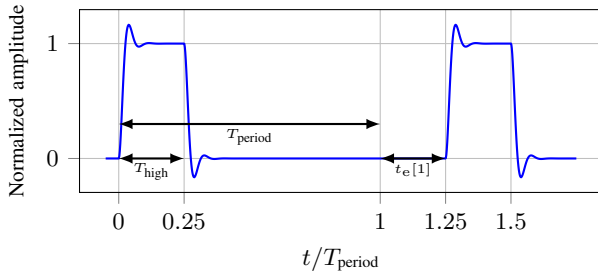


Fig. 1. Exemplary pulse signal modeled according to Equation 2. Note that every pulse is offset by an individual time-error $t_e[n]$.

Pulse signals complement sine wave reference signals by enabling *absolute* time synchronization. Typically, a so called 1 Pulse Per Second (1 PPS) signal with a T_{period} of 1 second is used. For example, when using a GPSDO as a 1 PPS source, the rising edge of the signal coincides with the Coordinated Universal Time (UTC) second. When a measurement device is accurately synchronized to full seconds using a 1 PPS signal, less precise mechanism, e.g. the Network Time Protocol (NTP) or a GPSDO's serial output, can be used to achieve absolute synchronization to UTC.

C. Reference Signal Measurement

Reference signal generators are purpose-built to provide highly stable signals and thus contain high-grade oscillators. These easily outperform those of laboratory measurement equipment and attempting to judge the stability of a reference signal using a measurement device with an inferior clock would defeat the purpose of the measurement. Therefore, the quality of reference signals is gauged by directly comparing two reference signals, eliminating the need for a highly-precise measurement clock.

To compare two sine signals of the same (or potentially different) frequency $x_{\text{sine},1}(t)$ and $x_{\text{sine},2}(t)$ (cf. Equation 1), the difference between their phase errors $\Delta\varphi(t)$ must be measured:

$$\Delta\varphi(t) = \varphi_{e,1}(t) - \varphi_{e,2}(t)$$

From this, the associated time error $\Delta t_{\text{sine}}(t)$ can be computed:

$$\Delta t_{\text{sine}}(t) = \frac{\Delta\varphi(t)}{2\pi f_r} \quad (3)$$

The comparison of two pulse signals $x_{\text{pulse},1}(t)$ and $x_{\text{pulse},2}(t)$ (cf. Equation 2) requires to determine the difference between their respective time errors $\Delta t_{\text{pulse}}[n]$:

$$\Delta t_{\text{pulse}}[n] = t_{e,1}[n] - t_{e,2}[n]$$

As *absolute* time synchronization requires both signal types, a reference signal measurement system should compare both signal types of two reference sources simultaneously.

II. STATE-OF-THE-ART OF MEASUREMENT SYSTEMS

TWO reference signal measurement architectures currently enjoy widespread use. The Dual Mixer Time Difference (DMTD) method is used for sinusoidal signals and the Time Interval Counter (TIC) technique is employed for pulse signals.

A. Time Interval Counter

A TIC is a digital circuit used to measure the time difference $\Delta t_{\text{pulse}}[n]$ between two (or more) pulse signals' rising edges. A basic implementation relies on a high-frequency digital clock, which is gated by digital circuitry responsible for pulse detection. The clock cycles between rising edges are counted to determine $\Delta t_{\text{pulse}}[n]$. Therefore, a TIC's resolution and accuracy depends on its digital clock. [3]

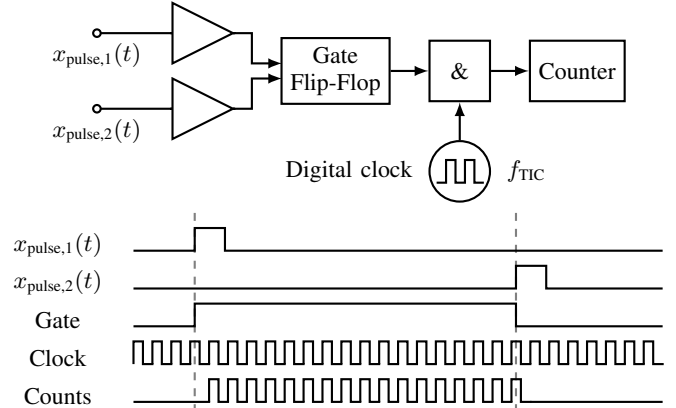


Fig. 2. Non-interpolating Time Interval Counter block diagram and signal timing graph. Note that the TIC's precision depends on its digital clock frequency f_{TIC} .

Figure 2 illustrates the operation of a non-interpolating TIC. The time resolution can be significantly improved at the cost of increased system complexity by implementing an interpolating TIC [4].

B. Dual Mixer Time Difference

The original DMTD method utilizes an analog, discrete circuit to measure the phase difference $\Delta\varphi(t)$ between two sine waves with (almost) identical frequency [5].

Fundamentally, the time difference between the sine waves' zero-crossings is measured using a TIC. However, instead of using the original reference signal at frequency f_r , which would require a highly accurate TIC with a high-frequency digital clock, the sine wave reference signal is down-converted to ease the constraints on the TIC. Figure 3 shows a typical DMTD block diagram illustrating this principle.

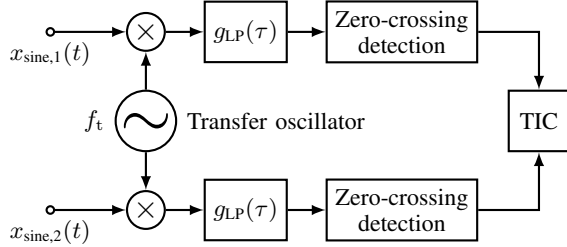


Fig. 3. Dual Mixer Time Difference block diagram.

Real-valued down-conversion with an analog mixing circuit and a transfer oscillator at frequency f_t is employed to down-shift the reference signal from frequency f_r to a very low intermediate frequency, the so-called beat frequency $f_b = |f_r - f_t|$. A low-pass filter $g_{LP}(\tau)$ is applied to eliminate interfering signal components (image frequency and up-converted Direct Current (DC) bias) and to reduce the noise bandwidth, resulting in the beat signal:

$$\begin{aligned} x_{\text{beat}}(t) &= \{x_{\text{sine}}(t) \cdot \sin(2\pi f_t t)\} * g_{LP}(\tau) \\ &= \{\sin(2\pi f_r t + \varphi_e(t)) \cdot \sin(2\pi f_t t)\} * g_{LP}(\tau) \\ &= \sin(2\pi f_b t + \varphi_e(t)) \end{aligned} \quad (4)$$

Its phase error term $\varphi_e(t)$ is identical to that of the original signal $x_{\text{sine}}(t)$ prior to down-conversion (cf. Equation 1).

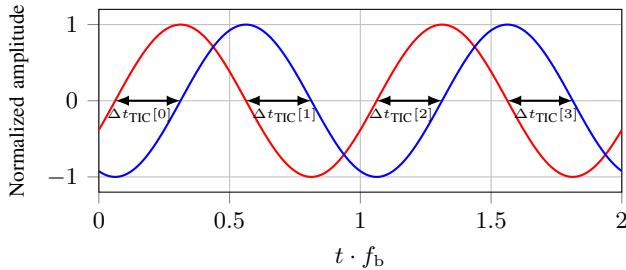


Fig. 4. Exemplary Dual Mixer Time Difference beat signals after down-conversion and low-pass filtering (cf. Equation 4). Note the two zero-crossings per period and the time-difference between consecutive zero-crossings $\Delta t_{\text{TIC}}[n]$, which is measured using a TIC.

Figure 4 illustrates the resulting beat signals, which will be fed to a TIC to gauge the time difference between their zero-crossings $\Delta t_{\text{TIC}}[n]$. The time error of the original signal can be computed as follows:

$$\Delta t_{\text{sine}}[n] = \frac{f_r}{f_b} \cdot \Delta t_{\text{TIC}}[n]$$

As can be concluded from Figure 4, the beat frequency determines the amount of zero-crossings and thus measurements per second ($2f_b$). It also dictates the heterodyne factor $\frac{f_r}{f_b}$ that quantifies the resolution gain over the TIC's native resolution (see above Equation). [1]

III. DIGITAL SIGNAL PROCESSING APPROACH

THE presented TIC and DMTD measurement techniques all rely on custom hardware setups and mixed-signal processing, requiring comprehensive know-how and integration effort to build a precise measurement device.

Instead of building custom measurement hardware, commercial measurement gear equipped with Analog-to-Digital Converters (ADC) to sample the reference signals and subsequent Digital Signal Processing (DSP) to perform the time-difference measurement could be used. This novel idea was published only recently¹ by Sherman and Jördens [7] as well as us [8], with this paper being an extension of our initial contribution.

Both parties describe measurement systems that utilize inexpensive Software Defined Radios (SDR) as general-purpose sampling platforms with built-in DSP capabilities and extensive programmability. However, the described algorithms are hardware-independent and can be implemented with any sampling platform that enables real-time or offline access to the sampled data.

A. DSP for Sine Wave Reference Signals

The sine wave DSP algorithm and its analog DMTD counterpart share the same core principle, namely the use of frequency down-conversion and subsequent phase measurement. However, the DMTD relies upon real-valued down-conversion, requiring zero-crossing detection for phase-measurement. Thereby, both measurement rate and resolution are restricted according to the chosen beat frequency f_b (see Section II-B).

This significant limitation is overcome by the DSP algorithm's use of complex down-conversion of the real-valued input signals (at sampling frequency f_s). A Numerically Controlled Oscillator (NCO) at frequency f_t is utilized as transfer oscillator. A low-pass filter $g_{LP}[m]$ is required to suppress potentially interfering signal components, i.e. image and up-converted DC bias.

We suggest choosing $f_t = f_r$, to result a beat frequency $f_b = 0$.² The measured signal's phase error $\varphi_e[n]$ is then equal to the phase angle of the complex signal. Otherwise, the phase angle contribution of f_b must be subtracted, which may be necessary, if the NCO is unable to exactly synthesize the required f_t . See Equations 5 and 6 for an analytic description.

$$\begin{aligned} z_{\text{sine}}[n] &= \left\{ x_{\text{sine}}(f_s n) \cdot e^{-j2\pi \frac{f_t}{f_s} n} \right\} * g_{LP}[m] \\ &= \left\{ \sin\left(2\pi \frac{f_r}{f_s} n + \varphi_e[n]\right) \cdot e^{-j2\pi \frac{f_t}{f_s} n} \right\} * g_{LP}[m] \\ &= e^{j2\pi \frac{f_b}{f_s} n} \cdot e^{j\varphi_e[n]} \end{aligned} \quad (5)$$

$$\varphi_e[n] = \arg\{z_{\text{sine}}[n]\} - \arg\left\{e^{j2\pi \frac{f_b}{f_s} n}\right\} \quad (6)$$

The algorithm yields a valid $\varphi_e[n]$ measurement for every sample of the input data (band-limited by $g_{LP}[m]$). Depending on the intended application, all output samples can be used, e.g. to compute the phase noise power-spectral density. Alternatively, the sample rate can be decreased by means of decimation (i.e. low-pass filtering and down-sampling) to

¹ Mochizuki et al. published an ADC-based measurement system in 2007. However, their implementation is still a custom-hardware mixed-signal DMTD system that uses an ADC instead of a TIC. [6]

² Sherman and Jördens [7] suggest a non-zero beat frequency f_b without giving an explanation for this choice. We assume this to be adopted from the real-valued processing performed by analog DMTD systems. Although a small, non-zero f_b shouldn't affect the measurement, $f_b = 0$ is the logical choice if complex-valued down-conversion is used.

facilitate long-term measurements with enhanced precision due to reduced noise bandwidth.

However, the computed phase error is only relative to the NCO that is implicitly driven by the sampling clock, which is inadequate to gauge high-performance reference oscillators. To compare two reference sources against each other, their complex signals can be divided, yielding a complex residual signal. See Figure 5 for an illustration of the algorithm.

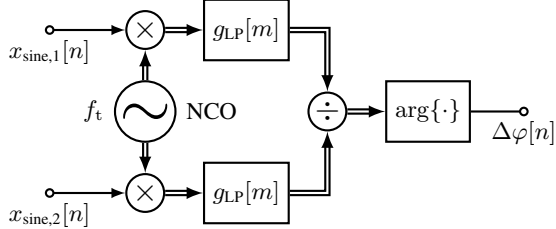


Fig. 5. Sine reference signal DSP algorithm block diagram. Note that single lines denote real-valued signals and double lines indicate complex signals.

The relevance of phase measurement is not limited to reference signals for synchronization. The IEEE Standard C37.118.1-2011 [9] addresses synchronous phasor measurements for power grids. Its non-normative Annex C defines a measurement algorithm, which is also based on complex down-conversion in the digital domain.

While synchronous phasor measurements must provide fast response times, our approach is tuned for high precision by applying rigorous baseband filtering with very high stopband attenuation. Furthermore, our approach employs dual-signal comparison (cf. Figure 5), which can improve the measurement precision for 10 MHz signals by up to an order of magnitude, as explained in [7].

B. DSP for Pulse Reference Signals

As described in Section I-B, pulse reference signals are best used as trigger events, wherefore the signal amplitude must exceed a defined threshold. To check for this with an ADC-based system, each sample's value could be compared against said threshold. However, this naïve approach would only provide a time resolution limited to the inverse of the sample rate f_s .

A simple TIC as described in Section II-A only possesses binary high/low information of a pulse signal. In contrast, a sampled version of the same pulse holds valuable amplitude information that can be used to interpolate the exact location of the signal edge exceeding the threshold level.

We suggest the following estimation algorithm to determine the exact edge location (see Figure 6 for an illustration based on a signal synthesized according to Section I-B):

- 1) Coarsely locate the rising/falling edge by applying a Schmitt-Trigger³ to the input signal at native sample rate. This provides an observation window with a configurable number of samples.
- 2) Increase the sample density within the observation window in order to approximate the edge location by low-pass interpolation (e.g. zero-padding the spectrum).

³Due to hysteresis thresholding, the Schmitt-Trigger provides highly reliable edge detection even in the presence of noise.

- 3) Ascertain the fractional sample index of the trigger event by linear interpolation.

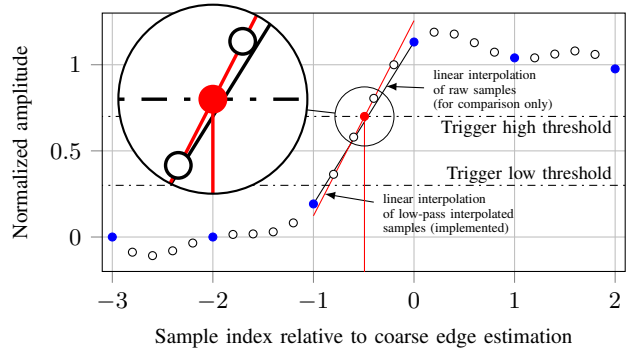


Fig. 6. Illustration of pulse signal edge estimation algorithm combining low-pass interpolation and linear interpolation. Plot shows sampled edge synthesized using Equation 2 (blue) and low-pass interpolated samples (black, hollow). Note how the low-pass interpolation improves the accuracy of the subsequent linear interpolation.

IV. SOFTWARE DEFINED RADIO SOLUTION

SDRs are mixed-signal measurement platforms typically used for RF applications. They are highly configurable, programmable and usually offer DSP capability on a Field Programmable Gate Array (FPGA) out of the box. Although most SDRs rely on local oscillators and analog up/down-conversion to achieve a wide range of selectable RF bands, some offer direct baseband access to their ADCs and/or Digital-to-Analog Converters (DAC).

The baseband DSP of SDRs supports Digital Up/Down-Conversion (DUC/DDC) and decimators/interpolators to enable configurable sample rates. Figure 7 illustrates a typical baseband DSP chain [10].

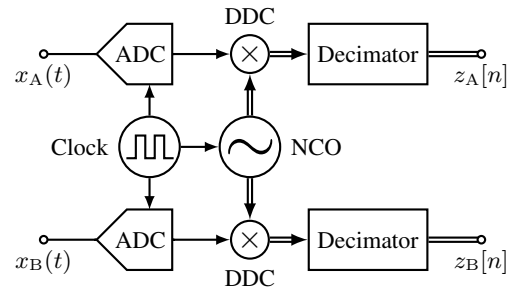


Fig. 7. Real-mode baseband DSP chain of typical direct-conversion SDR receiver. Note that when processing complex input data, no separate DDC is performed. The decimator block uses low-pass filtering and downsampling to adjust the output sample rate, as the ADCs' sample rate is fixed. Single lines denote real-valued signals, whereas double lines indicate complex signals.

To simultaneously measure both reference signal types, an SDR with 4 synchronous ADC channels that can be directly accessed is required. Preferably, it also supports real-mode baseband DSP as depicted in Figure 7.

Regardless of our choice for a specific SDR platform, we expect our suggested measurement technique to be applicable to a wide range of devices, not even limited to SDRs, since the algorithms described in Section III are hardware-agnostic. However, the widespread availability of SDRs and their built-in support for DSP primitives makes them a prime platform for implementation, enabling a comparatively cheap and easy to handle hardware solution.

A. USRP Measurement Hardware

The Universal Software Radio Peripheral (USRP) developed by Ettus Research LLC constitutes a flexible SDR platform, which is actively used within the academic community for a wide variety of communication or measurement scenarios. The entry level USRP N210 costs less than \$2,000 and features a dual-channel ADC and a dual-channel DAC interfaced by an FPGA. Although the N210 can be equipped with various RF front-ends, called daughterboards, the \$80 LFRX board enables direct baseband access to the dual-channel 14-bit ADC, also implementing the DSP chain illustrated in Figure 7.

The DDC is implemented using a Coordinate Rotation Digital Computer (CORDIC) fixed-point algorithm [11] and the decimator relies upon a Cascaded Integrator Comb (CIC) [12] filter with a final two-stage halfband Finite Impulse Response (FIR) filter [13] to steepen the overall frequency response. The combined filters enable integer decimation factors up to 500.

The N210 uses a Gigabit Ethernet connection to stream sampled data to a Personal Computer (PC) serving as a measurement host. The link's maximum data rate is insufficient to transfer the ADC's 100 Mega Samples (MS) per second data stream, necessitating a minimal decimation factor of 4 (for 16-bit sample streaming) or 2 (for 8-bit sample streaming).

A single, unsynchronized USRP N210 is sufficient to measure only one signal type. However, if both sine and pulse signals are to be evaluated as depicted in Figure 8, a dual USRP setup must be employed to reach the required count of 4 coherently sampled channels.

We rely on a Multiple-Input Multiple-Output (MIMO) cable to achieve inter-device clock synchronization, but strict synchronicity is only required if signals are to be compared across the USRPs. Both signals of each type are sampled on the same dual-channel ADC to improve sampling coherency.

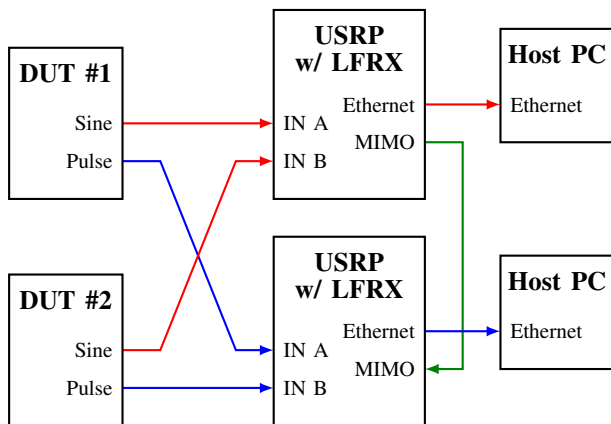


Fig. 8. Schematic of the USRP hardware setup required to measure the sine and pulse signals of 2 Devices Under Test (DUT). To evaluate only one signal type, a single, unsynchronized USRP is sufficient. Actually, strict synchronicity is only required if a cross-device signal comparison is desired.

B. Real-time Measurement Software

A real-time measurement software is implemented to significantly reduce the amount of data that need to be stored to disk compared to an off-line processing implementation. The latter would require a 200 MByte/s data stream to be stored,

which would imply a tremendous storage volume for long-term measurements.

Sine Signal Processing: A real-time implementation of the sine DSP algorithm described in Section III-A is supported by the USRP's DSP engine out of the box (compare Figures 5 and 7). Minimal programming effort on the host PC is required to configure the down-conversion and decimation DSP blocks appropriately.

Although the down-conversion and decimation filter algorithms (CORDIC and CIC) are implemented in 24-bit fixed-point arithmetic [14], the CIC filter offers only as little as 53 dB of stopband attenuation [12]. Therefore, we implemented single-precision floating-point down-conversion and FIR-based decimation on the host PC, so both DSP implementations can be directly compared (see Section V-A). Additionally, the host decimator can be used in conjunction with the FPGA DSP, if a decimation factor higher than the latter's limit of 500 is desired.

The host DSP is implemented in the C programming language and optimized by using the Single Instruction Multiple Data (SIMD) vector extensions of modern x86 processors. This enables real-time processing with 25 MS/s, providing better than 120 dB stop band attenuation of the FIR low-pass filter. Since 4 interleaved data streams must be processed in parallel (2 streams with an I/Q-pair each), vectorization can be realized efficiently. The host FIR decimator supports compile-time configuration of stage count, decimation factors, and FIR coefficients, so the target sample rate can be chosen according to the use scenario.

For our measurements, a default of 3 stages with decimation factor 10 was chosen as a trade-off between resulting bandwidth (20 kHz, 3 dB) and data rate (0.4 MByte/s), to enable long-term measurements without losing high-frequency phase noise information.

Pulse Signal Processing: The pulse DSP algorithm from Section III-B cannot be implemented on board the USRP without significant modification of its FPGA code. To avoid time-consuming and intricate FPGA development, we implemented the algorithm on the host PC using double-precision floating-point arithmetic and a low-pass interpolation factor of 20. No Single Instruction Multiple Data (SIMD) optimization effort was undertaken, since the interpolation is only performed for a limited number of samples, depending on the pulse signal's T_{period} . Finally, only the interpolation result is stored to disk, resulting in a negligible data rate and minimal storage volume.

Software Implementation: The USRP device family is supported by a wide variety of software development systems, including LabVIEW, MATLAB and GNU Radio. However, all of them lack an important feature vital to synchronized multi-USRP measurements. The User Datagram Protocol (UDP) used for sample transport between USRP and host PC is an unreliable transport layer protocol and is as such prone to packet loss. If packet loss occurs, the affected samples are lost and leave a zero-length gap in the sample stream, causing multiple streams to be out-of-sync.

To mitigate packet loss, we use proprietary USRP software

based on the USRP Hardware Driver (UHD) C++ library. If packet loss is detected, the stream is zero-padded appropriately to ensure a gap-free sample stream. Using a zero-copy ring buffer, this sample stream is accessed from multiple threads, distributing the load of sample reception and processing (i.e. computationally demanding FIR decimation). This also relaxes the real-time processing requirements, because the ring buffer allows for a considerable data processing delay.

To further reduce the likelihood of packet loss, we employ a customized minimal Linux system with optimized network interface settings (large Direct Memory Access buffer and improved interrupt coalescing) that successfully demonstrated zero packet loss within a week of continuous measurement on a 2011 laptop PC⁴.

C. Post-processing Software

As the real-time USRP software only performs limited pre-processing and data reduction, the actual evaluation is performed in a separate post-processing step. This approach was chosen in order to evaluate recorded data in multiple ways. The implemented post-processing focuses on the examined references' relative long-term drift.

First, the downmixed sine signal data is passed through additional high-attenuation FIR decimators to reduce its sample rate to 1 sample per second. Subsequently, the phase difference between both sine signals is computed using complex division (cf. Figure 5), unwrapped, and translated into a time error (see Equation 3).

The pulse signal pre-processing already produced interpolated edge times, so only the difference of both signals' rising edges is computed.

The Allan Variance is the standard statistical analysis method used in the field of frequency and time metrology [15]. Its aim is the description of random instabilities and the discrimination of the various modulated noise types that occur in oscillators (e.g. flicker and white noise) [16]. Unfortunately, its design makes it immune to constant offset and linear drift, both of which are detrimental to the *absolute* and *relative* synchronization of measurement devices. It is insufficient to use only the Allan Variance, if the synchronization-specific characteristics of an oscillator are to be considered.

Therefore, to determine the long-term drift of both signal types, a 1st order polynomial least-squares fit is applied. The resulting estimated linear drift can be used to adjust most frequency standards that usually provide a mechanism to slightly tune the generated frequency.

Complementary to above linear drift estimation, we use Savitzky-Golay filters [17]. These apply least-squares, moving-window, arbitrary-order polynomial fitting to the input data, smoothing it according to the chosen window length and polynomial order. Additionally, the same polynomial can be used to differentiate the (smoothed) input data, which we rely upon to ascertain the short-term drift of the time

error within the configured observation window. We have empirically chosen 2nd order polynomials to obtain a linear differentiation result.

V. MEASUREMENT PERFORMANCE EVALUATION

FOR the performance evaluation of our SDR measurement setup, we chose the most widely used reference signal types, i.e. 10 MHz sine and 1 PPS signals. To determine the precision of such a system, generally the residual time-difference between two identical signals is measured, which are generated by power-splitting a single signal [6], [7].

Figure 9 shows the modified SDR setup used for the following measurements. The inputs of the USRPs were kept at half-scale level to avoid distortion and to ensure a good Signal-to-Noise Ratio (SNR).

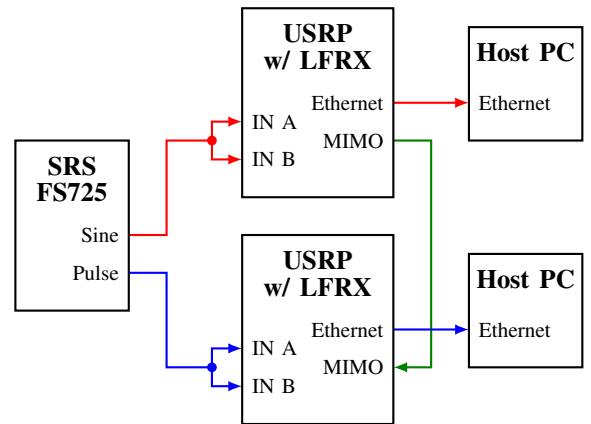


Fig. 9. Reference measurement setup. By using tee-connectors, each USRP receives virtually identical input signals with zero drift. This is exploited to evaluate the setup's inherent measurement accuracy.

A. Comparison of USRP and Host-based DSP

To compare the performance of both sine DSP implementations described in Section IV-B, we made multiple 1 hour measurements with different decimation factors n_{decim} and computed the SNR of the residual complex signal after division (cf. Figure 5).

TABLE I
SNR-COMPARISON OF USRP-BASED AND HOST-BASED 10 MHz DSP

n_{decim}	SNR CIC (dB)	SNR FIR (dB)	Δ_{SNR} (dB)
10	69.3	–	–
20	71.2	72.3	1.1
40	73.4	74.7	1.3
80	75.2	77.0	1.8
100	75.9	77.7	1.8
200	77.3	79.6	2.3
400	78.0	81.1	3.1
500	78.3	81.3	3.0

As can be seen from Table I, the host-based FIR decimation outperforms the FPGA-based alternative by up to 3 dB for high decimation factors. This is in good agreement with another 24 hour measurement that compares the Allan Deviation of both decimators for $n_{\text{decim}} = 500$ (see Figure 10).

Consequently, we suggest the use of host-based FIR decimation if maximum precision measurements are desired

⁴ The laptop form factor was chosen to build a compact measurement setup suitable for mobile use, e.g. outdoor GPSDO measurements. The PC is equipped with an i7-620M processor (2.66 GHz dual-core), 8 GiB random access memory, and a Gigabit Ethernet network interface.

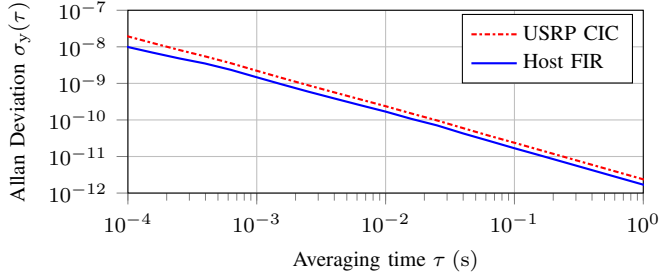


Fig. 10. Allan Deviation of FPGA-based CIC and host-based FIR decimators for $n_{\text{decim}} = 500$ during a 24 hour measurement. The Allan Deviation is displayed up to $\tau = 10^0$ s for better readability, but both curves' slope and difference continue until at least $\tau = 10^4$ s.

and its computational overhead is acceptable. We use the FIR decimator for our subsequent measurements to benefit from its superior precision.

B. Long-term Stability Measurement

To evaluate the SDR measurement system's precision and long-term stability, a continuous 95-hour measurement was taken. The resulting measurement data was evaluated as described in Section IV-C with a 2 hour Savitzky-Golay window length.

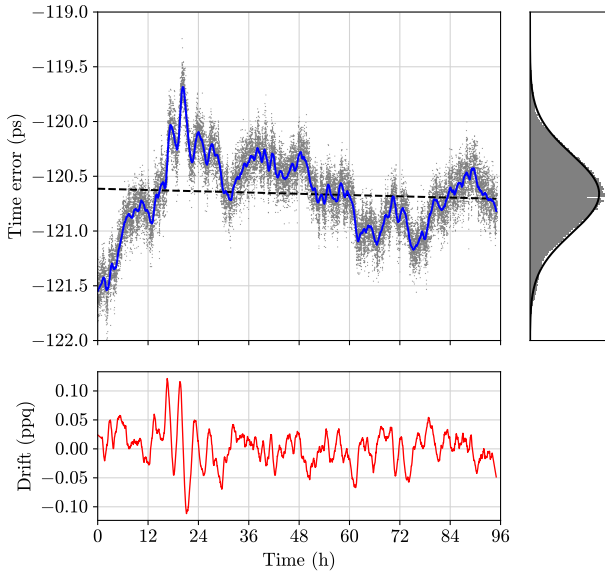


Fig. 11. 10 MHz signal reference measurement results. Figure shows raw time error (gray dots), linear drift fit (black dashed line), raw time error histogram (gray), normal distribution (black), Savitzky-Golay filtered time error (blue) and Savitzky-Golay differentiated short-time drift (red), the latter specified in parts-per-quadrillion (ppq, 10^{-15}). See Section IV-C for time error and drift definitions. Note the negligible linear drift ($-2.67 \cdot 10^{-19}$) and standard deviation ($\sigma = 359$ fs).

Figure 11 illustrates the 10 MHz signal measurement results. Despite the raw data's erratic appearance, its histogram reveals a normal distribution. The time error resolution is outstanding, with a 3σ accuracy of 1.08 ps, which corresponds to a phase angle resolution of 14.0 seconds of arc. These results can most likely be explained by the tremendous level of decimation, i.e. averaging, applied to the analog input signals.

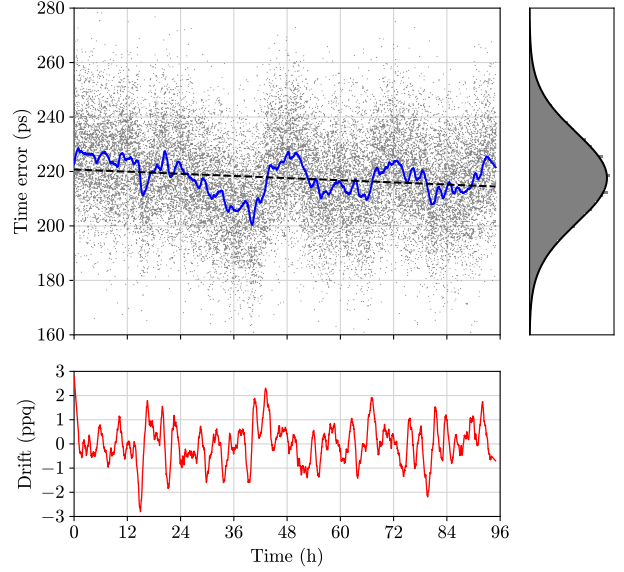


Fig. 12. 1 PPS signal reference measurement results. Figure shows raw time error (gray dots), linear drift fit (black dashed line), raw time error histogram (gray), normal distribution (black), Savitzky-Golay filtered time error (blue) and Savitzky-Golay differentiated short-time drift (red), the latter specified in parts-per-quadrillion (ppq, 10^{-15}). See Section IV-C for time error and drift definitions. Note the minimal linear drift ($-1.83 \cdot 10^{-17}$) and standard deviation ($\sigma = 16.60$ ps).

Figure 12 depicts the 1 PPS signal measurement results. Although significantly worse than the 10 MHz values, the 3σ time error resolution of 50 ps is still excellent, considering the high level of interpolation applied to the 25 MS/s input data (i.e. 40 ns of sample spacing).

TABLE II
10 MHz AND 1 PPS REFERENCE MEASUREMENT RESULTS

	10 MHz	1 PPS
σ	359 fs	16.6 ps
μ	-121 ps	218 ps
Linear drift	$-2.67 \cdot 10^{-19}$	$-1.83 \cdot 10^{-17}$

As can be concluded from Table II, both signal types' time errors show a comparatively high average value. Since a constant difference is irrelevant for our intended drift measurements, we did not investigate possible sources. However, different propagation delays are a likely explanation, since 120 ps correspond to only 2.4 cm of RG58 coax cabling.

If absolute measurement values are desired, further system calibration efforts beyond the scope of this paper become necessary.

C. Comparison with DMTD, TIC, and SDR Systems

A direct comparison from a synchronization-centric point of view of DMTD and TIC systems with our SDR solution would be highly interesting. However, we do not have DMTD or TIC hardware at our disposal, necessitating us to limit our comparison to published standard performance data, i.e. Allan Variance (DMTD) or standard deviation (TIC), respectively. Regrettably, this rules out long-term stability considerations (cf. Figure 11, Figure 12, and Section IV-C).

10 MHz Signal: Figure 13 uses the Allan Variance to compare the 10 MHz signal measurement performance of multiple DMTD and both SDR systems. Although our SDR measurement performs slightly worse than most analog DMTD systems for small τ , it outperforms all of them for $\tau \gg 10^3$ s.

The results of Sherman and Jördens are not directly comparable, because they employ a maximum likelihood time-domain optimization algorithm to determine the instantaneous frequency $\dot{\varphi}_e(t)$ (cf. Equation 1), assuming a linear phase drift during a variable observation window (see Appendix A of their paper [7]). This approach reduces the signal’s wideband noise and therefore improves its signal-to-noise ratio, decreasing the Allan Variance.

However, Sherman’s algorithm will distort the spectral characteristics of the signal, if the instantaneous frequency is not constant within the entire window. Particularly for long observation durations (Sherman chose $\tau \approx 10^3$ s), a constant $\dot{\varphi}_e(t)$ cannot be unconditionally assumed.

We avoid any such distortions, by using only spectrum-preserving post-processing prior to the computation of the Allan Variance, i.e. low-pass decimation with relatively high cut-off frequencies ($f_{c,3\text{dB}} \approx 0.8 f_{\text{Nyquist}}$). Additionally, our investigation of decimation on the host PC using floating-point arithmetic shows a 3 dB precision gain over Sherman’s use of the USRP’s built-in fixed-point DSP (see Section V-A). Therefore, we consider our algorithm a more general and more accurate approach.

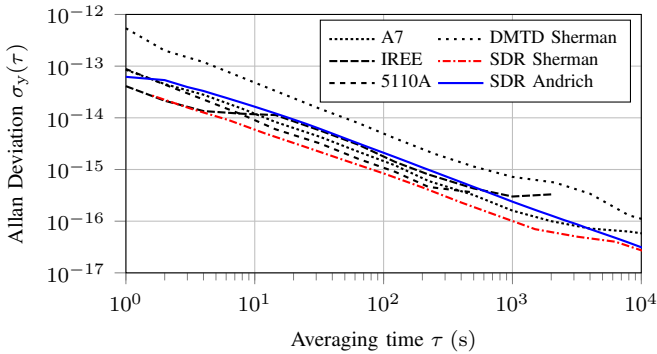


Fig. 13. Allan Deviation of different 10 MHz measurement systems, namely three DMTD systems (black lines, graphically extracted from [18]), an unknown DMTD system used for comparison by Sherman [7], and both SDR-based systems. Note that the SDR solutions perform comparably to DMTD hardware. Sherman’s SDR results were post-processed using an averaging interval of $\tau \approx 10^3$ s. Therefore, their results are not comparable to ours (see Section V-C for details).

1 PPS Signal: Table III lists the standard deviations σ of multiple TIC implementations capable of 1 PPS measurement, mostly taken from a comparison published by Szplet et al. [19]. The performance of our SDR system is comparable to that of FPGA-borne solutions (same order of magnitude). However, it is entirely software-based and therefore avoids the integration effort required to build a measurement system using only FPGA hardware. Since we are the first to publish such a solution [8], there are no references with other SDR-based 1 PPS measurements available for comparison.

TABLE III
MEASUREMENT PERFORMANCE OF TIME INTERVAL COUNTERS

Ref., Year	Platform	Method	σ (ps)
[19] 2013	FPGA	Equivalent coding line	6
[20] 2014	FPGA	Four-phase clock, Time coding line	150
[19] 2016	FPGA	Multi-edge coding in independent coding lines	6
[19] 2016	FPGA	Equivalent coding line	4.5
This work	SDR	Low-pass and linear interpolation	16.6

D. Comparison with Laboratory Measurement Equipment

Instead of specialized DMTD or TIC gear, general purpose laboratory measurement hardware can be relied upon for reference signal analysis. We have identified two devices to be used in a long-term stability comparison, namely a Rohde & Schwarz FSUP Signal Source Analyzer and a Tektronix DPO7254 Digital Sampling Oscilloscope. Similar devices should be available in any well-equipped RF laboratory, although results for other units will most likely vary.

Signal Analyzer: The Rohde & Schwarz FSUP combines phase noise testing and spectrum analysis features in a single \$100,000 class device. It supports various phase noise measurement scenarios, including the measurement of 2 Devices Under Test (DUT) against each other, which is required for a comparison with our SDR solution. The double DUT measurement mandates control over at least one oscillator’s frequency by supplying a tuning voltage, as is typical for Voltage Controlled Oscillators (VCO). However, reference signal generators cannot be tuned like VCOs and the FSUP fails to lock its phase detector without tuning control.

Unfortunately, the FSUP does not enable the comparison of 2 reference signal generators as is supported by our SDR system. Although the FSUP is solicited as phase noise tester, we assume that the use case was not envisioned or intended by the designers, which is unfortunate, considering the device’s cost. Consequently, the split-signal measurement to characterize the device’s precision (cf. Section V, Figure 9) is not possible, either.

Digital Sampling Oscilloscope: The Tektronix DPO7254 is a 4 channel, 40 Giga Samples (GS) per second Digital Sampling Oscilloscope (DSO) with 2.5 GHz of analog bandwidth. It is a \$30,000 class device with various built-in measurement features, including those required to measure the phase difference of sinusoidal signals and the time difference (i.e. delay) between the edges of pulse signals. Thus, it supports the features required for a comparison with our SDR system out of the box.

We realized the split-signal measurement from Figure 9, using a single DPO7254 instead of 2 synchronized USRP N210. The DPO’s channels used for 1 PPS measurement operated at the full 2.5 GHz bandwidth for maximum time resolution, while the 10 MHz measurement channels were band-limited at 20 MHz to suppress wide-band noise. In order to gain an insight into the DPO’s measurement abilities, we compared 3 different configurations for 96 hours, each:

- Simultaneous measurement of **10 MHz** and **1 PPS** signals as enabled by our SDR setup. Full quad-channel sample rate of **10 GS/s** and 500 ns observation window with 40-fold interpolation, as trade-off between both signal types' precision.
- Only the **10 MHz** signal, but at **20 GS/s** dual-channel sample rate. Peak observation window length of $50 \mu\text{s}$ without interpolation to minimize measurement dead-time.
- Only the **1 PPS** signal, but at **20 GS/s** dual-channel sample rate. Highest possible interpolation factor of 200 with 50 ns observation window length to maximize time resolution.

We employed the built-in phase and/or delay measurement features of the DPO7254 and read out the values over Ethernet using the VXI-11 protocol, yielding exactly one measurement per second by using the 1 PPS signal to trigger the DSO⁵. Table IV lists the standard deviation σ , mean μ , and linear drift of the 3 measurements outlined above, as well as our USRP results from Table II for comparison.

Because different cables were used for both measurements (the DPO7254 has BNC inputs; the USRP N210 has SMA ports) the different μ values are non-significant and subject to calibration, anyway. All linear drifts are smaller than the corresponding σ values and therefore negligible.

TABLE IV
PERFORMANCE COMPARISON BETWEEN SDR AND DSO

		10 MHz	1 PPS
USRP N210 4 channel 25 MS/s	σ	359 fs	16.6 ps
	μ	-121 ps	218 ps
	Linear drift	$-2.67 \cdot 10^{-19}$	$-1.83 \cdot 10^{-17}$
DPO7254 4 channel 10 GS/s	σ	128 ps	30.5 ps
	μ	120 ps	-1.75 ps
	Linear drift	$-8.89 \cdot 10^{-17}$	$-3.70 \cdot 10^{-19}$
DPO7254 2 channel 20 GS/s	σ	107 ps	32.1 ps
	μ	44.7 ps	-8.60 ps
	Linear drift	$4.93 \cdot 10^{-17}$	$-1.87 \cdot 10^{-18}$

As an additional statistical comparison of the 10 MHz measurements, Figure 14 illustrates their Allan Variances. Similarly to the σ values, the USRP measurement setup outperforms the DPO by more than 2 orders of magnitude. Although the DPO uses 400 (or even 800) times the sample rate of the USRP, this advantage is nullified by the DPO's substantial measurement dead-time (zero vs. $\geq 99.995\%$) and higher noise bandwidth (0.8 Hz vs. 20 MHz), compared to the USRP.

Although the Allan Variation is usually relied upon to characterize sinusoidal oscillators, we also use it to statistically compare the 1 PPS measurements (see Figure 15). Here, the USRP and the DPO are much closer, but the USRP still leads by a factor of 2. Curiously, the DPO's precision deteriorates when switching from 10 GS/s to 20 GS/s. This could be caused

⁵Note that although the DPO7254 supports multiple measurements per second, it only refreshes its value display twice in that interval. Curiously, the same limitation applies to the VXI-11 value readout. Therefore, we did not attempt to increase the sample rate for the dual-channel 10 MHz measurement by using an external trigger signal faster than the 1 PPS. For both other measurements, the 1 PPS signal must be used as trigger, anyway.

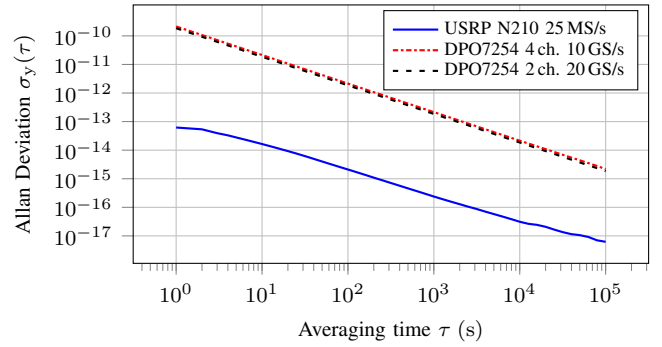


Fig. 14. Allan Deviation of 10 MHz signal long-term measurements. The USRP outperforms the DPO by more than 2 orders of magnitude. Note that the dual-channel DPO measurement enables a slight improvement over its quad-channel counterpart.

by the DPO internally interleaving 2 ADCs to double the sample rate at the potential cost of increased noise and jitter.

It seems quite impressive that an inexpensive SDR outperforms a DSO, which provides more than 200 times the analog bandwidth (i.e. time resolution) and 400 (or even 800) times the sample rate. This is facilitated by the versatility of the Software Defined Radio platform, allowing to implement customized algorithms that achieve vast precision gains. It also proves that our algorithm's combination of low-pass and linear interpolation (cf. Section III-B) is well suited for the precise estimation of signal edges.

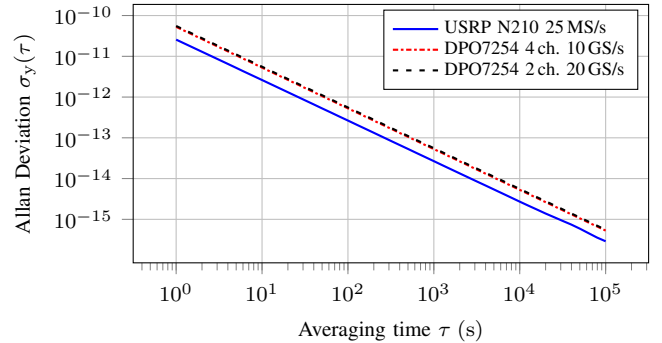


Fig. 15. Allan Deviation of 1 PPS signal long-term measurements. Note that the USRP outperforms the DPO by 3 dB, despite its inferior analog bandwidth (i.e. time resolution) and sample rate, compared to the latter.

VI. CONCLUSIONS

WE presented a system for high-precision measurement and analysis of reference signals, based on commercial off-the-shelf Software Defined Radio (SDR) hardware. As SDR platforms are quite common in research laboratories, it seems likely to use them also for instrumentation in a cost-efficient way. In this paper, we described how to analyze the stability of sine and pulse reference signals on the basis of the Universal Software Radio Peripheral (USRP) N210 by Ettus Research LLC.

Sine reference signals were digitally down-converted to baseband for the analysis of phase deviations. For this purpose, out-of-the-box algorithms natively provided by common SDRs can be used as a basis. As an extension, we demonstrated that the precision of the Digital Signal Processing chain (which is normally provided by SDRs using fixed-point arithmetic)

can be improved by custom software, running on the host PC. Using floating-point arithmetic in connection with Single Instruction Multiple Data (SIMD) vector extensions of modern processors, real-time performance can be provided even on moderate hardware.

The analysis of pulse reference signals was realized by a software trigger running on the host PC that precisely locates the trigger event time, i.e. where the slope passes a certain threshold. Clearly, due to limited sample rate an adequate post-processing was needed. Therefore, low-pass interpolation for increasing the sample density was applied, followed by a linear interpolation to ascertain the fractional sample index of the trigger event.

Using the USRP N210 SDR-platform, a measurement precision (standard deviation) of 0.36 ps and 16.6 ps was obtained for 10 MHz and 1 PPS reference signals, respectively, which is in the same order of magnitude compared to state-of-the-art methods such as the Dual Mixer Time Difference (DMTD) method and the Time Interval Counter (TIC).

Furthermore, joint and individual measurements of 10 MHz and 1 PPS signals with a Digital Sampling Oscilloscope (Tektronix DPO7254) showed that our proposed inexpensive SDR-based approach outperforms high-grade laboratory equipment by more than 2 orders of magnitude for 10 MHz phase estimation and by factor 2 for 1 PPS edge detection. The SDR is also less bulky, cheaper, and more power efficient.

The proposed SDR-setup can be used out of the box, e.g. to check the integrity or rather for calibration of reference sources against each other. It is suitable even for long-term measurements (days or weeks) and inherently provides a consistent storage of data. A similar SDR-based approach was recently proposed by Sherman and Jördens [7] for the analysis of sine signals, only. However, such an SDR-based system being capable of joint sine and pulse reference signal analysis is not found in literature, so far.

ACKNOWLEDGEMENTS

This work was supported by the Free State of Thuringia and the European Social Fund.

REFERENCES

- [1] W. Riley and D. A. Howe, "Handbook of Frequency Stability Analysis," NIST, 7 2008. [Online]. Available: <https://www.nist.gov/publications/handbook-frequency-stability-analysis>
- [2] M. Siccardi, D. Rovera, and S. Romisch, "Delay measurements of PPS signals in timing systems," in *2016 IEEE International Frequency Control Symposium (IFCS)*, 5 2016, pp. 1–6.
- [3] J. Kalisz, "Review of methods for time interval measurements with picosecond resolution," *Metrologia*, vol. 41, no. 1, p. 17, 2004. [Online]. Available: <http://stacks.iop.org/0026-1394/41/i=1/a=004>
- [4] R. Szplet, D. Sondej, and G. Grzeda, "Subpicosecond-resolution time-to-digital converter with multi-edge coding in independent coding lines," in *2014 IEEE International Instrumentation and Measurement Technology Conference (I2MTC) Proceedings*, 5 2014, pp. 747–751.
- [5] D. W. Allan and H. Daams, "Picosecond Time Difference Measurement System," in *29th Annual Symposium on Frequency Control*, 5 1975, pp. 404–411.
- [6] K. Mochizuki, M. Uchino, and T. Morikawa, "Frequency-Stability Measurement System Using High-Speed ADCs and Digital Signal Processing," *IEEE Transactions on Instrumentation and Measurement*, vol. 56, no. 5, pp. 1887–1893, 10 2007.
- [7] J. A. Sherman and R. Jördens, "Oscillator metrology with software defined radio," *Review of Scientific Instruments*, vol. 87, no. 5, p. 054711, 2016.
- [8] C. Andrich, A. Ihlow, W. Kotterman, N. Beuster, and G. D. Galdo, "Using software defined radios for baseband phase measurement and frequency standard calibration," in *2017 IEEE International Instrumentation and Measurement Technology Conference (I2MTC)*, 5 2017, pp. 1–5.
- [9] "IEEE Standard for Synchrophasor Measurements for Power Systems," *IEEE Std C37.118.1-2011 (Revision of IEEE Std C37.118-2005)*, pp. 1–61, 12 2011.
- [10] P. Cruz, N. B. Carvalho, and K. A. Remley, "Designing and Testing Software-Defined Radios," *IEEE Microwave Magazine*, vol. 11, no. 4, pp. 83–94, 6 2010.
- [11] J. E. Volder, "The CORDIC Trigonometric Computing Technique," *IRE Transactions on Electronic Computers*, vol. EC-8, no. 3, pp. 330–334, 9 1959.
- [12] E. Hogenauer, "An economical class of digital filters for decimation and interpolation," *IEEE Transactions on Acoustics, Speech, and Signal Processing*, vol. 29, no. 2, pp. 155–162, 4 1981.
- [13] L. Doolittle, "Filtering and Decimation by Eight in an FPGA for SDR and Other Applications," 2010. [Online]. Available: <http://recycle.lbl.gov/~ldoolitt/halfband/filter.pdf>
- [14] "USRP DDC Verilog source code," Ettus Research LLC. [Online]. Available: https://github.com/EttusResearch/fpga/blob/UHD-3.10.1.1/usrp2/sdr_lib/ddc_chain.v#L108
- [15] "IEEE Standard Definitions of Physical Quantities for Fundamental Frequency and Time Metrology – Random Instabilities," *IEEE Std 1139-2008 (Revision of IEEE Std 1139-1999)*, pp. 1–50, 2 2009.
- [16] J. Rutman and F. L. Walls, "Characterization of frequency stability in precision frequency sources," *Proceedings of the IEEE*, vol. 79, no. 7, pp. 952–960, 7 1991.
- [17] A. Savitzky and M. J. E. Golay, "Smoothing and Differentiation of Data by Simplified Least Squares Procedures," *Analytical Chemistry*, vol. 36, no. 8, pp. 1627–1639, 1964.
- [18] L. Sojdr, J. Cermak, and G. Brida, "Comparison of high-precision frequency-stability measurement systems," in *IEEE International Frequency Control Symposium and PDA Exhibition Jointly with the 17th European Frequency and Time Forum, 2003. Proceedings of the 2003*, 5 2003, pp. 317–325.
- [19] R. Szplet, P. Kwiatkowski, Z. Jachna, and K. Rózyć, "An eight-channel 4.5-ps precision timestamps-based time interval counter in fpga chip," *IEEE Transactions on Instrumentation and Measurement*, vol. 65, no. 9, pp. 2088–2100, 9 2016.
- [20] R. Szplet, P. Kwiatkowski, K. Rózyć, M. Sawicki, and Z. Jachna, "Modular time interval counter," in *2014 European Frequency and Time Forum (EFTF)*, 6 2014, pp. 494–497.